RSC Advances

Volume 1 | Number 1 | Jan 2013 | Pages 1–100

RSC Advances

www.rsc.org/advances

ROYAL SOCIETY OF CHEMISTRY

ROYAL SOCIETY OF CHEMISTRY

www.rsc.org/advances

High performance solid state supercapacitor based on 2-mercapto pyridine redox-mediated gel polymer

Kanjun Sun[a,b*]; Miaomiao Dong[b]; Enke Feng[b]; Hui Peng[b]; Guofu Ma[b*]; Guohu Zhao[a]; Ziqiang Lei[b]

[a]College of Chemistry and Environmental Science, Lanzhou City University, Lanzhou 730070, China.

[b]Key Laboratory of Eco-Environment-Related Polymer Materials of Ministry of Education, Key Laboratory of Polymer Materials of Gansu Province, College of Chemistry and Chemical Engineering, Northwest Normal University, Lanzhou 730070, China.

E-mail: sunkj@lzcu.edu,cn, magf@nwnu.edu.cn

Abstract

A novel gel polymer polyvinyl alcohol-orthophosphoric acid-2-mercapto pyridine (PVA-H_3PO_4-PySH) is prepared through introducing redox-mediated 2-mercapto pyridine into polyvinyl alcohol-orthophosphoric acid host, and a solid state supercapacitor is fabricated using the gel polymer as electrolyte and separator, activated carbons as electrodes. The mechanical properties tests show the PVA-H_3PO_4-PySH gel polymer has excellent stretching and bending properties. The electrochemical properties of the supercapacitor are investigated by cyclic voltammetry, galvanostatic charge-discharge and electrochemical impedance spectroscopy. Surprisingly, 447% of electrode specific capacitance (1128 F g^{-1}) and energy density (39.17 Wh kg^{-1}) are increased while introducing PySH as the redox mediator in PVA-H_3PO_4 gel polymer. The supercapacitor with PVA-H_3PO_4-PySH gel polymer shows excellent capacitance retention of 80% for over 1000 cycles. Simultaneously, the ionic conductivity of the gel polymer electrolyte increased by 92% up to 22.57 mS cm^{-1} compared to that of PVA-H_3PO_4 system. These improved performances are owed to the redox reaction between 2-mercapto pyridine (PySH) and 2,2'-bipyridine (PySSPy) redox couples in PVA-H_3PO_4-PySH gel electrolyte that make the

---

[*] Corresponding author. Tel.: +86 931 7975121; fax: +86 931 7975121.
E-mail addresses: sunkj@lzcu.edu,cn (Kanjun Sun), magf@nwnu.edu.cn (Guofu Ma).

supercapacitor combines the double-layer characteristic of carbon-based supercapacitors and the faradaic reactions characteristic of batteries energy-storage processes.

Keywords: Doped gel polymer, Gel electrolyte, solid state supercapacitor

1. Introduction

Flexible devices are a mainstream direction in modern electronics and related multidisciplinary fields [1-3]. Concerning flexible capacitors and batteries, the current research is mainly focused on the fabrication of flexible electrode materials [4-6], however, electrolyte development is also a critical factor for attaining highly flexible devices [7-8]. The development of flexible energy devices even soft robots has quickly increased the requirement of soft electrolyte with mechanical robustness and facile ion or solute transport [9-11]. Therefore, for the special configuration design and fabrication of novel energy storage devices, a thin and flexible layer of gel polymer electrolytes (GPEs) is considered to be the most effective geometry because of the intrinsic properties of GPEs, such as thin-film forming ability, high reliability, flexibility, facile designing, separator-free as well as the relatively high ionic conductivity [12-14]. Compared with the conventional energy storage devices using liquid electrolytes, the energy storage devices based on GPEs don’t require high standard safety encapsulation materials and thus their geometry shape is variable, which may bring new design opportunities for energy storage devices in the future wearable electronics field [15-16].

In order to prepare high-performance GPEs, several polymer matrix materials have been developed and investigated in recent years, including poly(ethylene oxide) (PEO), poly(vinyl alcohol) (PVA), poly(methyl methacrylate) (PMMA), poly(acrylonitrile) (PAN), poly(vinylidene fluoride) (PVDF). Among these polymers, PVA is a good candidate for GPEs because of its excellent chemical stability, mechanical property, high ability to form transparent film and nontoxicity [12, 17-18].

Moreover, for the purpose of further improving the electrochemical performance of the GPEs, some modification methods have been utilized, such as the additions of the basic or acidic salt to enhance the conductivity because of the high dynamics of hydroxyl or proton (e.g., KOH and

H_2SO_4) [12, 18], and the incorporation of the redox mediator to bring the additional pseudocapacitance by the quick reversible redox reaction [19-21]. Senthilkumar *et al.* [22] reported that 57.2% of specific capacitance and of energy density was increased while introducing Na_2MoO_4 (sodium molybdate) as the redox mediator in PVA-H_2SO_4 gel electrolyte due to the redox reaction between Mo(VI)/Mo(V) and Mo(VI)/Mo(IV) redox couples in PVA-Na_2MoO_4-H_2SO_4 gel electrolyte. The pseudocapacitive effect of p-benzenediol in PVA-H_2SO_4 were investigated by Yu et al. [23], the specific capacitance of electrode reached 474.29 F g^{-1} (−0.5 to 0.5 V), which was much higher than that of the PVA-H_2SO_4 system in the same conditions. Wu et al. [24] reported that p-phenylenediamine could been used as a redox intermedium in KOH electrolyte, and the supercapacitor with KOH + PPD electrolyte has a much higher electrode specific capacitance (605.225 F g^{-1}) than the one with conventional KOH electrolyte (144.037 F g^{-1}) at the same current density of 1 A g^{-1}. Besides, the other redox mediators, such as potassium ferricyanide [25] and methylene blue [26] have been added into the gel electrolyte to enhance the capacitive performance of carbon-based supercapacitors. Although the above research enhanced the capacitive performance of supercapacitors, little significant research on 2-mercapto pyridine type redox mediator in the gel electrolyte have been attempted.

The stable and reversible redox reactions of 2-mercapto pyridine (PySH) have been research and application in the field of organic synthesis and biological sensors [27-29]. Here, we introduce the PySH into the PVA-H_3PO_4 gel polymer electrolyte for the activated carbon-based supercapacitor. Because of intrinsic redox states and quick reversible faradaic reactions, the PVA-H_3PO_4-PySH gel electrolyte simultaneously possesses higher ionic conductivity, additional pseudocapacitance and good stability, it is expected that the electrochemical performance of the electrolyte and the corresponding supercapacitor can be remarkably improved.

2. Experimental

2.1. Materials

Polyvinyl alcohol (PVA, Aladdin Co., China, molecular weight 44.05 MW, alcoholysis: 99.8-100%), H_3PO_4 (Tianjin Baishi chemical co., China), 2-mercaptopyridine (PySH, Shanghai Saen Chemical Technology Co., China), Activated carbon (AC, Shanghai Sino Tech Investment

Management Co., China). All other chemical reagents were in analytical grade.

2.2. Preparation of gel polymer

Gel polymer electrolyte was prepared in solution-casting method by modifying the procedure from the previous literature [30]. First, 1 g PVA was dissolved in 10 mL distilled water with agitation at 80 °C for 2 h to form a homogeneous and low-viscous solution. Then, 10 mL aqueous solution containing H_3PO_4 (2.0 g) and PySH (0-0.20 g) was added to the above solution with constant stirring, and it was kept until formation of a gel-like solution. Finally, the resultant mixture was poured into a to 90 mm plastic petri dish, and the dish was frozen at -25 °C for 12 h and thawed at room temperature for 12 h. The freeze-thaw cycles were repeated for 2 times to obtain the PVA-H_3PO_4-PySH gel polymer.

For comparison purpose, the gel polymer PVA-H_3PO_4 without PySH was also prepared under the same conditions.

2.3. Preparation of activated carbon electrode

Initially, powdered activated carbon, acetylene black and binder polytetrafluoroethylene (PTFE) aqueous solution in the weight ratio 80:10:10 was put in agate mortar and dispersed by 0.4 mL of *N*-methyl-2-pyrrolidone (NMP) to form a uniform slurry [31]. Further, the obtained slurry was coated on the stainless steel net (thickness = 0.06 mm) with an area of 1 cm^2 and dried at 60 °C for overnight. An AC electrode thus was obtained and the active material loading was (including acetylene black and polytetrafluoroethylene) to be 2.5 mg on each electrode.

2.4. Fabrication of supercapacitor

A two-electrode test supercapacitor was fabricated with a pair of the AC electrodes and stretchable gel polymer electrolyte in a sandwich configuration. The gel polymer simultaneously served as electrolyte and separator, and the two stainless steel nets with the electrode material were used as current collectors. The schematic diagram and model of supercapacitor are given in **Fig. 1** (a) and (b).

2.5. Characterizations

The mechanical performance of the gel polymer was tested via bending and stretching. The membrane of the gel polymer was cut into a ribbon of 0.7 cm width and 3.0 cm length and the deformation was caused under proper forces. Then the elongation at break is tested for PVA-H_3PO_4 and PVA-H_3PO_4-PySH gel polymers by microcomputer control electronic universal testing machine (WDW-2C) at the same thickness and extension rate of 5mm min^{-1}.

All electrochemical measurements were performed on an electrochemical workstation system (Model: CHI 660D, Shanghai Chen Hua Co., Ltd) using a two-electrode system under ambient conditions. The electrochemical properties of the supercapacitor were studied through CV at different scan rates from 5 to 50 mV s^{-1} and GCD test at different current densities from 0.5 to 5 A g^{-1} for potential of -1 to 1 V. Electrochemical impedance spectroscopy (EIS) was carried out at open circuit potential (OCP) by applying ac potential with 5 mV amplitude in the frequency ranges from 0.1 Hz to 10^5 Hz. Measurement of cycle-life stability were performed using computer controlled cycling equipment (LAND CT2001A, Wuhan, China). The specific capacitances (C, F g^{-1}) of the supercapacitor and electrode (C_s, F g^{-1}) were evaluated from charge-discharge curves according to the following equation [32]:

$$C = (I \times \Delta t) / (\Delta V \times m_{ac}) \qquad (1)$$

$$C_s = 4 \times C \qquad (2)$$

Energy density (E, Wh kg^{-1}), equivalent series resistance (ESR, Ω) and power density (P, kW kg^{-1}) of the supercapacitor were calculated according to the following equations [32-33]:

$$E = [(C \times (\Delta V)^2) / 2] \times (1000 / 3600) \qquad (3)$$

$$ESR = iR_{drop} / (2 \times I) \qquad (4)$$

$$P = (\Delta V)^2 / (4 \times ESR \times m_{ac}) \qquad (5)$$

where I (A) is the discharge current, m_{ac} (g) is the weight of active material (including the acetylene black and the binder), Δt (s) is the discharge time, ΔV (V) is the operating voltage window of the supercapacitor, and iR_{drop} (V) is defined as the electrical potential difference between the two ends of a conducting phase during charging-discharging.

Besides, ionic conductivity of the gel polymer in the supercapacitor was also determined from impedance spectrum. The ionic conductivity (σ, S cm^{-1}) of gel polymer can be calculated by the following equation [31]:

$$\sigma = L / (R_b \times S) \quad (6)$$

where L (cm) is the distance between the two pieces of stainless steel net, R_b (ohm), obtained from the curves of EIS, is the bulk resistance, S (cm^2) is the contact area of the electrolyte film with stainless steel net during the experiment (manually measured for several times).

3. Results and discussions

3.1. Mechanical properties of gel polymer

The PVA-H_3PO_4-PySH gel polymer has excellent stretching and bending properties. It can be observed from **Fig. 2**(a) and (b), the gel polymer ribbon can be elastically stretched to about 2 times length than its original, and from **Fig. 2**(c) and (d), the gel polymer ribbon is easy twisted into a spiral and bent into a circle without fracturing. All the ribbons are able to quickly recover its original length and shape after the external force was removed which exhibit outstanding mechanical properties.

The data of tensile elongation at break are obtained as 311.93% of PVA-H_3PO_4 and 392.17% of PVA-H_3PO_4-PySH gel polymers. We can infer that the doping 2-mercapto pyridine could improve the flexible and tensile properties.

3.2. Ionic conductivity of gel polymer

Fig. 3 shows the effect of the amount of PySH on ionic conductivity of the gel polymer. As can be seen, when the amount of PySH is less than 0.17 g, the ionic conductivity rises quickly and reaches the highest value of 22.57 mS cm^{-1} with the PySH amount of 0.17 g, but, when the PySH content beyond 0.17 g, the ionic conductivity gradually decreases with the increase of PySH content, which means that the ionic conductivity of PVA-H_3PO_4 gel polymer can be improved with the appropriate doping amount of PySH. It is probably because of the quick reversible redox processes triggered by PySH, making the ionized PySH provide more valid ions transferring through the free volume in the polymer host, therefore, the ionic conductivity of PVA-H_3PO_4 gel polymer is improved. When the PySH amount is less, such as less than 0.17 g, PySH function as redox shuttle cannot realize well, and the conductivity of the gel polymer is smaller. However, higher PySH content will lead to the aggregation of free ions and the crystallization of PySH in

PVA-H_3PO_4 system, which impeded the ions transport and induced the decrease of the ionic conductivity [34]. Therefore, 0.17 g PySH is optimal content in PVA-H_3PO_4 gel polymer.

3.3. Cyclic voltammetry measurements

Cyclic voltammetry for the supercapacitor with PVA-H_3PO_4 and PVA-H_3PO_4-PySH gel electrolytes at scan rate of 10 mV s^{-1} in the potential window range from -1 to 1 V are shown in **Fig. 4**(a). Almost rectangular behavior without visible redox peaks is observed for PVA-H_3PO_4 that infers the capacitance is stored by an accumulation of electrolyte ions between the electrode|electrolyte interfaces which is known as electric double layer capacitance [32]. In contrast, while using PVA-H_3PO_4-PySH as electrolyte and separator, a pair of well-defined and strong redox peaks (centered at -0.25 and 0.25 V and corresponding to the oxidation and reduction of PySH and PySSPy, respectively) appears in CV curves. The probably processes of redox reactions are presented in **Fig. 5 [**29], this reaction make the supercapacitor has faradaic reactions characteristic of batteries [35]. Since the peak potential differences of the redox pair are small and the voltammetric response on the positive sweeps is symmetric to its counterpart on the negative sweep, a reversible redox process occurs in this electrolytic system [24]. As we know, pseudocapacitive performance can be heightened by the redox reaction and consequently employed as an electrolyte material for supercapacitors. Obviously, the appearance of the redox peaks indicates that the addition of PySH enhances electrode's capacitive performance, which can be inferred from the areas of CVs [36].

Fig. 4(b) represents the CV curves for the supercapacitor based on PVA-H_3PO_4-PySH gel electrolyte at different scan rates. It is observed that CV curve area and the peak current rapidly increase with the increase of the scan rate from 5 to 50 mV s^{-1}. Moreover, a pair of redox peaks is still clearly observed even at a scan rate of 50 mV s^{-1}. The result reveals that the supercapacitor with PVA-H_3PO_4-PySH gel electrolyte has the reversible redox processes and good rate ability [37]. In addition, from the CV curves we can find that, as the scan rate increases, the potentials of the oxidation and reduction peaks shift to more positive and negative directions. This may be due to the limitation of the ion diffusion rate to satisfy electronic neutralization during the redox reaction [38].

3.4. Galvanostatic charge-discharge measurements

The galvanostatic charge-discharge curves for the supercapacitor with the PVA-H_3PO_4 and PVA-H_3PO_4-PySH gel electrolyte are shown in **Fig. 6**. Obviously, the charge-discharge time of the supercapacitor with PVA-H_3PO_4-PySH is much longer than that of the supercapacitor with PVA-H_3PO_4. On the other hand, from the charge-discharge curves detected in the potential range of 0 to 1 V, the supercapacitor with PVA-H_3PO_4-PySH gel electrolyte exhibits nonlinear charge-discharge behavior. The inclined parts in the charging potential and the discharging potential indicate a quick reversible redox reactions are occured in the charge-discharge process [23], which are consistent with the cyclic voltammograms in **Fig. 4**. Furthermore, the longer charge-discharge time, which may be due to the additional contribution of the PySH that has been interpreted aforementioned, reveals great improvement in the electrochemical performances of the supercapacitor with PVA-H_3PO_4-PySH gel electrolyte.

According to Eq. (2), for a charging-discharging current density of 0.5 A g^{-1}, discharging specific capacitance of the electrode for the supercapacitors with PVA-H_3PO_4 and PVA-H_3PO_4-PySH are determined to be 206 and 1128 F g^{-1}, respectively. Obviously, the C_s of the supercapacitor with PVA-H_3PO_4-PySH is larger than that of the supercapacitor with PVA-H_3PO_4 gel polymer. The electrode discharging specific capacitance for the supercapacitors with the PVA-H_3PO_4-PySH is increased by 922 F g^{-1} compared to the current PVA-H_3PO_4 system, indicating that the redox mediator PySH can greatly improve the capacitive property of the supercapacitor.

The charge-discharge curves of the supercapacitor with PVA-H_3PO_4-PySH gel polymer at various current densities of 0.5, 0.8, 1, 2, and 3 A g^{-1} are displayed in **Fig. 7**, and the C_s are calculated to be 1128, 825, 600, 368, and 300 F g^{-1}, respectively. As we can see, even when the current density is 3 A g^{-1}, the value of C_s is larger than that of the supercapacitor based on the PVA-H_3PO_4 gel polymer at lower density (206 F g^{-1} at 0.5 A g^{-1}). It indicates clearly that a supercapacitor with PVA-H_3PO_4-PySH gel electrolyte shows superior electrochemical behaviour. The better performances may be due to the quicker ions diffusion rate and more adequately electrode|electrolyte interfacial contact, which are enhanced by the PySH.

The energy and power densities were calculated from the galvanostatic charge-discharge at different current densities. According to Eqs. (3) and (5), energy density and power density are obtained and shown in **Fig. 8**. It is obviously that the supercapacitor with PVA-H_3PO_4-PySH gel polymer exhibit the highest energy density 39.17 Wh kg^{-1} at a power density of 250 W kg^{-1} and remain 10.42 Wh kg^{-1} at 1500 W kg^{-1}, while the energy density and power density for the supercapacitor with PVA-H_3PO_4 gel polymer is only 7.15 Wh kg^{-1} and 250 W kg^{-1}. The supercapacitor with PVA-H_3PO_4-PySH electrolyte has better electrochemical performances may be due to the pseudocapacitive contribution generated by the redox reactions of the redox mediator (PySH) in the supercapacitor system. Moreover, it is worth mentioning that the obtained maximum energy density of the supercapacitor with PVA-H_3PO_4-PySH is considerably higher than those of recently reported carbon-based supercapacitor using redox-mediated gel polymer as electrolyte, such as PVA-KOH-KI (7.80 Wh kg^{-1}) [19], PVA-KOH-PPD (82.56 Wh kg^{-1}) [24], PVA-H_2SO_4-PB (10 Wh kg^{-1}) [23] and PVA-KOH-$K_3[Fe(CN)_6]$ (57.94 Wh kg^{-1}) [25].

3.5. EIS technique

In order to investigate the electrochemical behavior at the electrode|electrolyte interface in detail, EIS measurements were employed at open circuit potential in the frequency range from 100 mHz to 100 kHz. The corresponding Nyquist impedance plots are shown in **Fig. 9**. The equivalent circuit used for fitting of the EIS plots in this work is shown in **Fig. 9** by ZSimpWin software [39, 40]. R_{ESR} is the equivalent series resistance (ESR), R_{CT} is the resistance of the electrode-electrolyte, C_{DL} is the constant phase element of double layer, W is the Warburg element. The fitted data for all circuit elements is shown in Table 1. A possible reason for insensitivity to varying voltage scan rates is a short and equal diffusion path length of the ions in the electrolyte, as evidenced by a short Warburg region on the Nyquist plots [41]. In the EIS curves, It can be seen that two gel polymers exhibit ideal electrochemical capacitance behavior, i.e., a small depressed semicircle at higher frequency, a small ~45° inclined line at middle frequency which is known as diffusive or warburg resistance of ions with electrode and imaginary parts of impedance at low frequency region are nearly linear. In addition, the supercapacitor with PVA-H_3PO_4-PySH not only has lower inner resistance (R_i, 8.735 Ω cm^2) calculated from the point of intersecting with the x-axis in the range of high frequency, but also possesses smaller interfacial charge transfer resistance (R_{ct}, 3.027 Ω cm^2), counting from the span of the single semicircle along the x-axis from high to low frequency region. Besides, *Rb*, the most important data used in the calculation formula of ionic conductivity, is obtained as follow: draw a tangent line going along the slope of EIS curves in the range of low frequency until intersect with *x*-axis. The point of intersection is the data we need. Clearly, the PySH additive enhances the interaction of electrolyte|electrode interface, which results in good electrochemical property for PVA-H_3PO_4-PySH gel electrolyte system.

3.6. Cycle-life testing

The stability of a supercapacitor for repetitious charge-discharge cycles is one of the most electrochemical performances for its practical application. Herein, the cycle life test is carried out at a constant charge-discharge current density of 1 A g^{-1} for 1000 cycles, and the plots of electrode specific capacitances of supercapacitors based on PVA-H_3PO_4 and PVA-H_3PO_4-PySH gel polymer as a function of charge-discharge cycles are depicted in **Fig. 10**. After 1000 charge-discharge cycles, the C_s of PVA-H_3PO_4 system decreases from 176 to 158 F g^{-1}, and the C_s of PVA-H_3PO_4-PySH system decreases from 600 to 480 F g^{-1}, still retains 89.7 % and 80.0 % of the initial capacitance, respectively. It can be concluded that a redox-active PySH doping not only can increase the C_s of supercapacitor, but also scarcely impede the stability of supercapacitors, indicating that the PVA-H_3PO_4-PySH gel polymer can be considered as promising electrolyte and separator in the application of high-energy supercapacitor.

4. Conclusions

In the present work, a novel redox mediator gel polymer PVA-H_3PO_4-PySH was prepared by adding redox additive PySH into PVA-H_3PO_4 gel polymer electrolyte, and a solid state supercapacitor was assembled using the gel polymer as electrolyte and separator, activated carbon as electrode. The supercapacitor with PVA-H_3PO_4-PySH gel polymer electrolyte simultaneously possesses high ionic conductivity (22.57 mS cm^{-1}), large electrode specific capacitance (1128 F g^{-1}), high energy density (39.17 Wh kg^{-1}), and excellent cycle life that maintains 80.0 % of the initial capacitance values after 1000 cycles. This result may be due to the fact that the redox reaction of PySH make the supercapacitor combines the double-layer characteristic of carbon-based supercapacitors and the faradaic reactions characteristic of batteries energy-storage processes. It is strongly believed that the PVA-H_3PO_4-PySH gel polymer can be considered as promising electrolyte and separator in the application of high-energy supercapacitor and the idea using redox mediator has a good prospect for improving the performances of supercapacitors.

Acknowledgments

We thank to the Science and Technology program of Gansu Province (NO. NO.1308RJZA295, 1308RJZA265), the Colleges and Universities Scientific Research Program of Gansu Province (2013B-069), the PhD Scientific Research starting Program of Lanzhou City University (LZCU-BS2013-11), the program for Changjiang Scholars and Innovative Research Team in University (IRT1177), Key Laboratory of Eco-Environment-Related Polymer Materials (Northwest Normal University) of Ministry of Education, and Key Laboratory of Polymer Materials of Gansu Province.

References

[1] K. Jost, C. R. Perez, J. k. McDonough, V. Presser, M. Heon, G. Dion Y. Gogotsi, Energy Environ Sci, 2011, **4**, 5060-5067.

[2] V. Presser, L. F. Zhang, J. J. Niu, J. McDonough, C. Perez, H. Fong, Y. Gogotsi, Adv. Energy Mater, 2011, **1**, 423-430.

[3] Z. B. Yang, J. Deng, X. L. Chen, J. Ren, H.S. Peng, Angew Chem Int Ed 2013, **52**, 13453-13457.

[4] X. Xiao, X. Peng, H. Y. Jin, T. Q. Li, C. C. Zhang, B. Gao, B. Hu, K. F. Huo, J. Zhou, Adv Mater, 2013, **25**, 5091-5097.

[5] A. Sumboja, C.Y. Foo, X. Wang, P.S. Lee, Adv Mater, 2013, **25**, 2809-2815.

[6] Y. P. Fu, X. Cai, H. W. Wu, Z. B. Lv, S. C. Hou, M. Peng, X. Yu, D. C. Zou, Adv Mater, 2012, **24**, 5713-5718.

[7] H. Li, Q. Zhao, W. Wang, H. Dong, D. S. Xu, G. J. Zou, H. L. Duan, D. P. Yu, Nano Lett, 2013, **13**, 1271-1277.

[8] C. W. Huang, C. A. Wu, S. S. Hou, P. L. Kuo, C. T. Hsieh, H. S. Teng, Adv Funct Mater, 2012, **22**, 4677-4685.

[9] J. H. Cho, J. Y. Lee, Y. Xia, B. S. Kim, Y. Y. He, M. J. Renn, T. P. Lodge, C. D. Frisbie, Nat Mater, 2008, 7, 900-906.

[10] S. A. Morin, R. F. Shepherd, S. W. Kwok, A. A. Stokes, A. Nemiroski, G. M. Whitesides, Science, 2012, **337**, 828-832.

[11] S. Zhang, K. H. Lee, C. D. Frisbie, T. P. Lodge, Macromolecules, 2011, **44**, 940-949.

[12] N. A. Choudhury, S. Sampathb, A. K. Shukla, Energ Environ Sci, 2009, **2**, 55-67.

[13] J. Reiter, J. Vondrak, J. Michalec, Z. Micka, Electrochim. Acta, 2006, **52**, 1398-1408.

[14] Md. A. B. H. Susan, T. Kaneko, A. Noda, M. Watanabe, J Am Chem Soc, 2005, 127, 4976-4983.

[15] F. Croce, G. B. Appetecchi, L. Persi, B. Scrosati, Nature, 1998, 394, 456-458.

[16] J. M. Tarascon, M. Armand, Nature, 2001, **414**, 359-367.

[17] V. K. Thakur, G. Ding, J. Ma, P. S. Lee, X. Lu, Adv Mater, 2012, **24**, 4071-4096.

[18] N. A. Choudhury, A. K. Shukla, S. Sampath, S. Pitchumani, J Electrochem Soc A, 2006, **153,** 614-620.

[19] H. J. Yu, J. H. Wu, L. Q. Fan, K. Q. Xu, X. Zhong, Y. Z. Lin, J. M. Lin, Electrochim Acta, 2011, **56**, 6881-6886.

[20] Y.J. Yin, J.J. Zhou, A.N. Mansour, X. Zhou, J Power Sources, 2011, **196**, 5997-6002.

[21] J. J. Zhou, J. S. Cai, S. R. Cai, X. Y. Zhou, A. N. Mansour, J Power Sources, 2011, **196**, 10479-10483.

[22] S. T. Senthilkumar, R. K. Selvan, J. S. Melo, C. Sanjeeviraja, Appl Mater Interfaces, 2013, **5**, 10541-10550.

[23] H. J. Yu, J. H. Wu, L. Q. Fan, Y. Z. Lin, K. Q. Xu, Z. Y. Tang, C. X. Cheng, S. Tang, J. M. Lin, M. L. Huang and Z. Lan, J Power Sources, 2012, **198**, 402-407.

[24] J. H. Wu, H. J. Yu, L. Q. Fan, G. G. Luo, J. M. Lin, M. L. Huang, J Mater Chem, 2012, **22**, 19025-19030.

[25] G. F. Ma, J. J. Li, K. J. Sun, H. Peng, J. J. Mu, Z. Q. Lei, J Power Sources, 2014, **256**, 281-287.

[26] F. D. Yu, M. L. Huang, J. H. Wu, Z. Y. Qiu, L. Q. Fan, J. M. Lin, Y. B. Lin, J Appl Polym Sci, 2014, **10**, 39783-39790.

[27] D. Perez-Quintanilla, I. D. Hierrl, M. Fajardo, I. Sierra, Micropor Mesopor Mat, 2006, **89**, 58-68.

[28] N. Kuwamura, K. Kitano, M. Hirotsu, Chem Eur J, 2011, **17**, 10708-10715.

[29] S. I. Naya, M. Teranishi, T. Isobeb, H. Tada, Chem Commun, 2010, **46**, 815-817.

[30] C. Yang, S. Hsu, W. Chien, J Power Sources, 2005, **152**,303-310.

[31] H. Y. Lee, S. M. Lee, Electrochem Comm, 2004, **6**, 465-469.

[32] X. Y. Lang, A. Hirata, T. Fujita, M. W. Chen, Nat Nanotechnol, 2011, **6**, 232-236.

[33] C. Z. Meng, C. H. Liu, L. Z. Chen, C. H. Hu, S. S. Fan, Nano lett, 2010, **10**, 4025-4031.

[34] P. Jannasch, Polymer, 2001, **42**, 8629-8635.

[35] S. Roldán, C. Blanco, M. Granda, R. Menéndez and R. Santamaría, Angew Chem Int Ed, 2011, **50**, 1699-1701.

[36] S. Chen, J. W. Zhu, X. D. Wu, Q. F. Han, X. Wang, ACS Nano, 2010, **4**, 2822-2830.

[37 H. Peng, G. F. Ma, J. J. Mu, K. J. Sun, Z. Q. Lei, J Mater Chem A, 2014, **2**, 17297-17301.

[38] J. W. Lee, T. Ahn, D. Soundararajan, J. M. Ko, J. D. Kim, Chem Commun, 2011, **47**, 6305-6307.

[39] M, D. Stoller, S, Park, Y, Zhu, J. An , R. S. Ruoff, Nano Lett, 2008, **8**, 3498–3502.

[40] R. Hastak, P. Sivaraman, D. Potphode, K. Shashidhara, A. Samui, Electrochim Acta, 2012, **59**, 296–303.

[41] W. Wang, S. R. Guo, I. Lee, K. Ahmed, J. B. Zhong, Z. Favors, F. Zaera, M. Ozkan, C. S. Ozkan, Scientific Reports, 2014, **4**, 1-9.

Figure captions:

Fig. 1. (a) Schematic diagram of fabricated supercapacitor; (b) Schematic representation for the supercapacitor model.

Fig. 2. Photographs of flexible PVA-H_3PO_4-PySH gel polymer.

Fig. 3. Ionic conductivity of PVA-H_3PO_4-PySH gel electrolyte with different contents of PySH.

Fig. 4. (a) CV curves for the supercapacitors with PVA-H_3PO_4 and PVA-H_3PO_4-PySH gel electrolytes at scan rate of 10 mV s^{-1}; (b) CV curves for the supercapacitor with PVA-H_3PO_4-PySH gel electrolyte at different scan rates from 5 mV s^{-1} to 50 mV s^{-1}.

Fig. 5. Representation of the redox processes in the electrode|electrolyte system (black, red and yellow correspond to carbon, nitrogen and hydrogen atoms)

Fig. 6. Galvanostatic charge-discharge curves of supercapacitors with PVA-H_3PO_4 and PVA-H_3PO_4-PySH gel electrolytes at a current density of 0.5 A g^{-1}.

Fig. 7. Galvanostatic charge-discharge curves of supercapacitors with PVA-H_3PO_4-PySH gel polymer at various current densities.

Fig. 8. Ragone plot related to energy and power densities of the supercapacitors with PVA-H_3PO_4 and PVA-H_3PO_4-PySH gel polymer electrolytes.

Fig. 9. EIS of supercapacitors with PVA-H_3PO_4 and PVA-H_3PO_4-PySH gel polymer electrolytes.

Fig. 10. Cycle-life of the supercapacitors with PVA-H_3PO_4 and PVA-H_3PO_4-PySH electrolytes in the long-term cycle at the charge-discharge current density of 4 A g^{-1}.

Table 1. Fitted equivalent circuit elements of PVA-H_3PO_4-PySH gel polymer electrolytes.

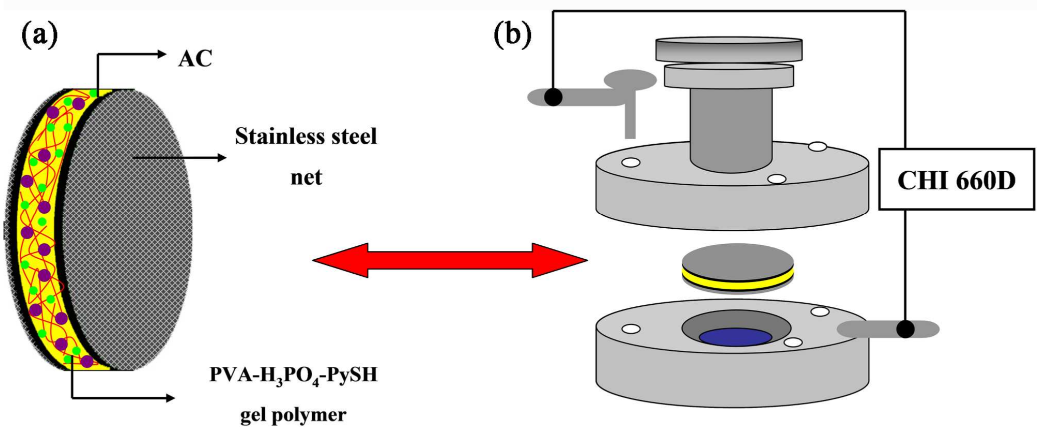

Fig. 1. (a) Schematic diagram of fabricated supercapacitor; (b) Schematic representation for the supercapacitor model.

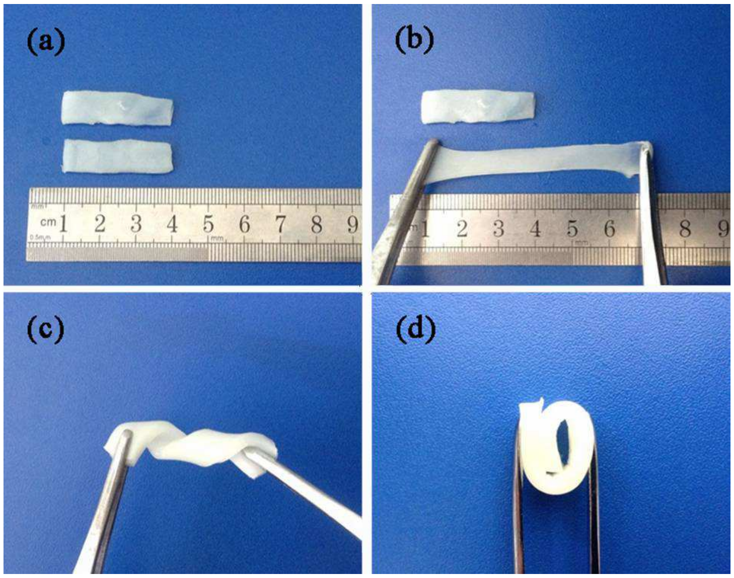

Fig. 2. Photographs of flexible PVA-H_3PO_4-PySH gel polymer.

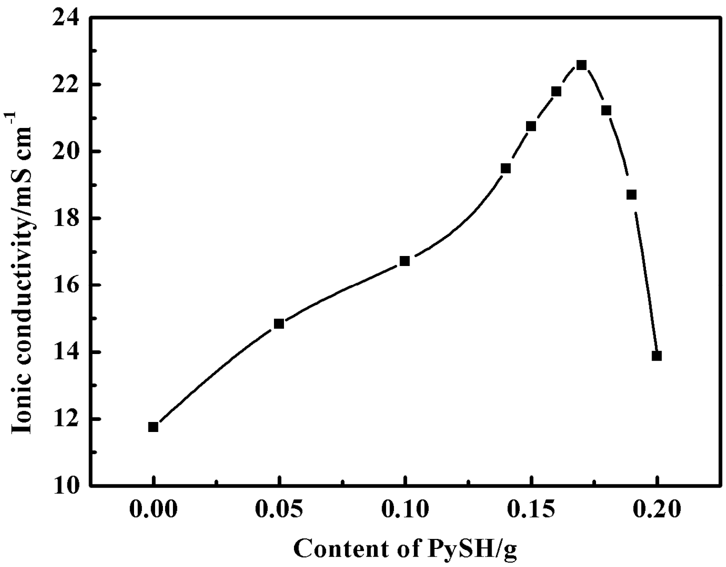

Fig. 3. Ionic conductivity of PVA-H_3PO_4-PySH gel electrolyte with different amounts of PySH.

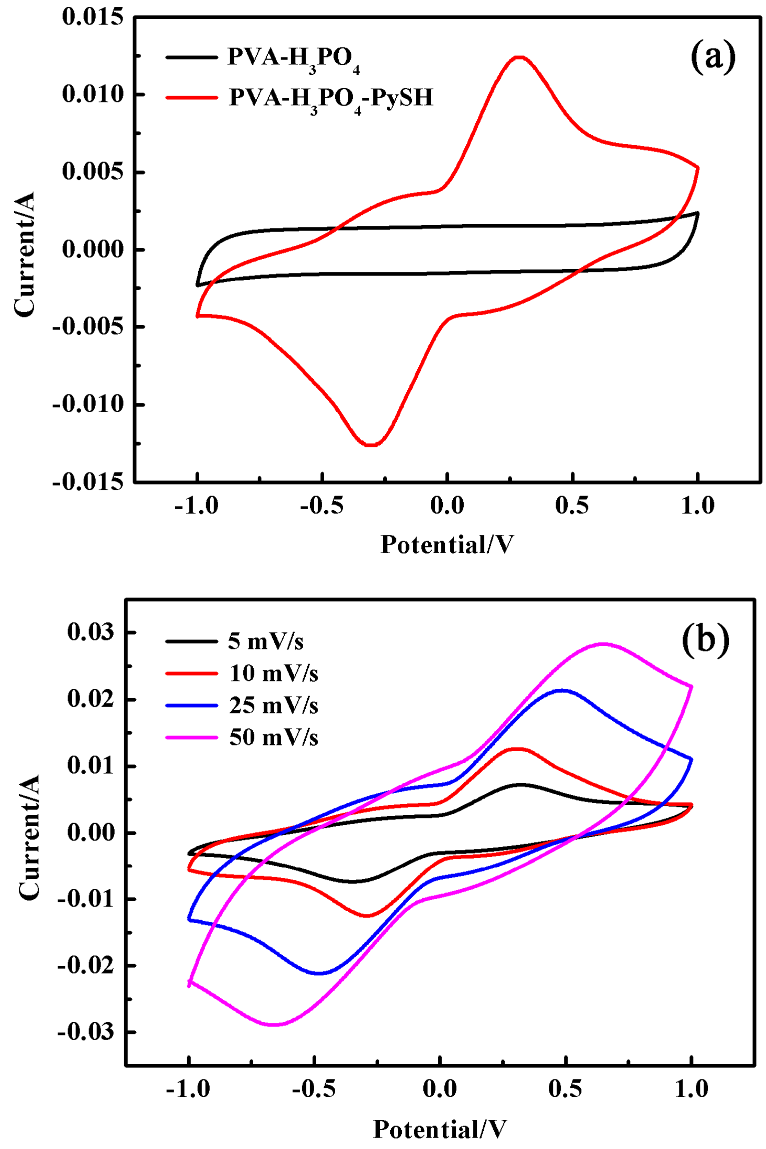

Fig. 4. (a) CV curves for the supercapacitors with PVA-H$_3$PO$_4$ and PVA-H$_3$PO$_4$-PySH gel electrolytes at scan rate of 10 mV s^{-1}; (b) CV curves for the supercapacitor with PVA-H$_3$PO$_4$-PySH gel electrolyte at different scan rates from 5 mV s^{-1} to 50 mV s^{-1}.

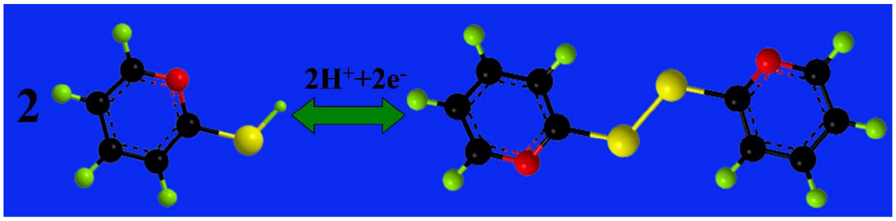

Fig. 5. Representation of the redox processes in the electrode|electrolyte system (black, red, yellow and green correspond to carbon, nitrogen, sulfur and hydrogen atoms).

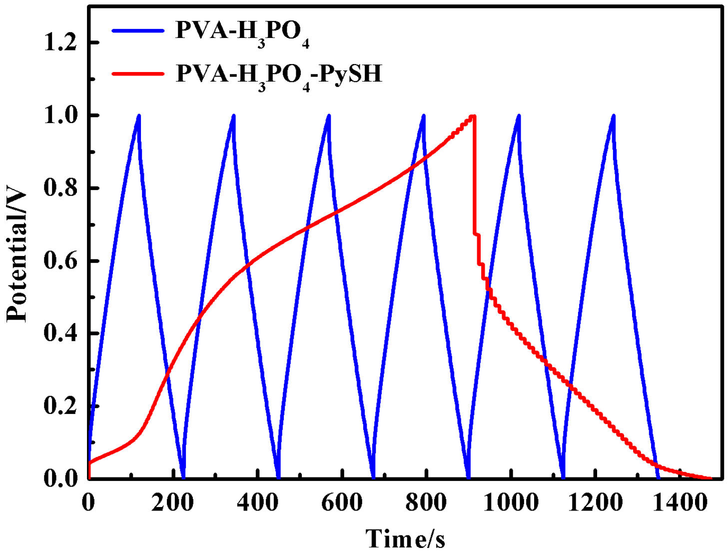

Fig. 6. Galvanostatic charge-discharge curves of supercapacitors with PVA-H_3PO_4 and PVA-H_3PO_4-PySH gel electrolytes at a current density of 0.5 A g^{-1}.

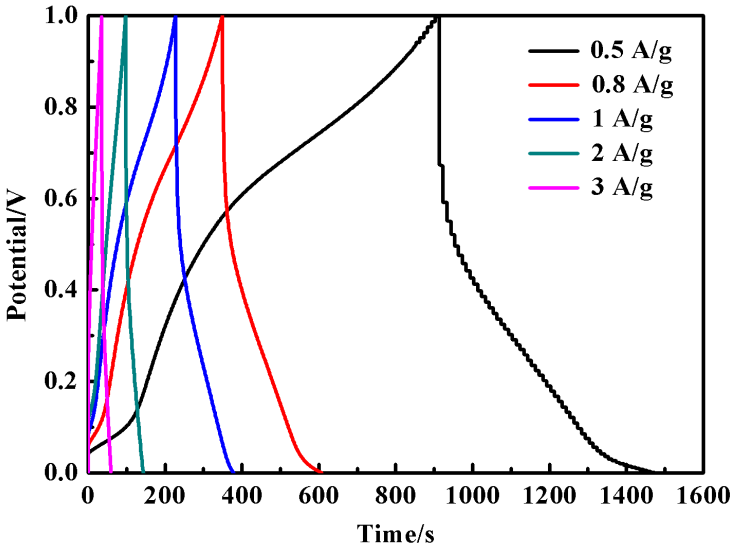

Fig. 7. Galvanostatic charge-discharge curves of supercapacitors with PVA-H_3PO_4-PySH gel polymer at various current densities.

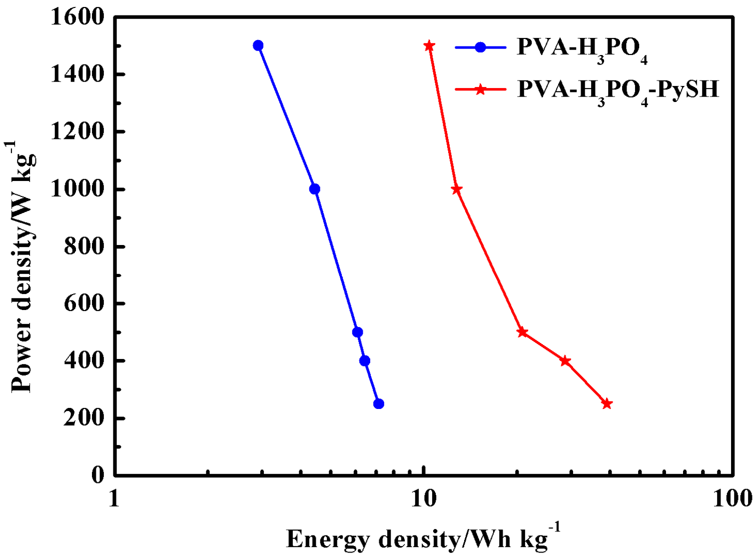

Fig. 8. Ragone plot related to energy and power densities of the supercapacitors with PVA-H$_3$PO$_4$ and PVA-H$_3$PO$_4$-PySH gel polymer electrolytes.

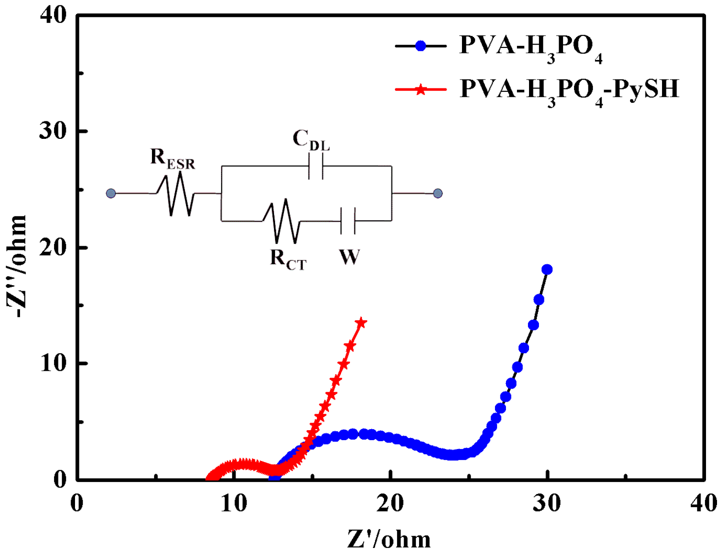

Fig. 9. EIS of supercapacitors with PVA-H_3PO_4 and PVA-H_3PO_4-PySH gel polymer electrolytes.

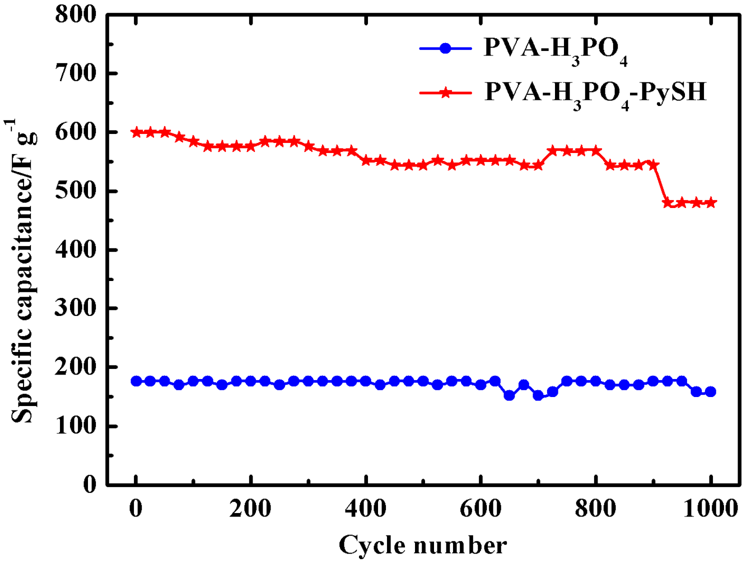

Fig. 10. Cycle-life of the supercapacitors with PVA-H$_3$PO$_4$ and PVA-H$_3$PO$_4$-PySH electrolytes in the long-term cycle at the charge-discharge current density of 4 A g^{-1}.

Table 1. Fitted equivalent circuit elements of PVA-H_3PO_4-PySH gel polymer electrolytes.

R_{ESR}	R_{CT}	C_{DL}	W
8.755Ω	2.792Ω	0.0001157	0.0983